ASSESSMENT OF DEFORESTATION DURING THE LAST DECADES IN ECUADOR USING NOAA-AVHRR SATELLITE DATA

Víctor González-Jaramillo, Andreas Fries, Rütger Rollenbeck, Jhoana Paladines, Fernando Oñate-Valdivieso and Jörg Bendix

With 8 figures, 2 tables and 1 supplement
Received 19 July 2015 · Accepted 7 June 2016

Summary: Human activities during the last decades provoked a notable reduction in global forest cover. Knowing that forest stands act as stock and sinks for carbon and other greenhouse gases, it is important to determine the existing forest cover at country level and to calculate annual deforestation rates. This work uses NOAA satellite images in a resolution of 1 km x 1 km to classify the surface of continental Ecuador in "forest" – "non-forest" pixels and to estimate the annual deforestation rate from 1986 to 2001 as well as from 2001 to 2008. The method is based on a decision tree algorithm that includes different spectral bands of the NOAA-AVHRR sensor and additional topographic and meteorological parameters. The results show that the total forest cover of continental Ecuador was reduced from 48.1 % in 1986 to 36.8 % in 2008. The calculated annual deforestation rates indicate that forest reduction increased during the last decade. The most affected area is the Coastal Lowland, due to the enhanced population pressure, followed by the Amazon Basin, not only caused by the governmental supported oil and mining industry, but also due to the uncontrolled timber extraction. The Andean Highland has been less affected, because the major parts of this region were deforested before, during the Pre-Columbian-Era.

Zusammenfassung: In den letzten Jahrzehnten führten menschliche Tätigkeiten zu einer deutlichen Abnahme der globalen Waldbestände. Da bekannt ist, dass Wälder als Speicher und Senken für Kohlenstoff und andere Treibhausgase dienen, ist es wichtig die noch existierenden Waldbestände einzelner Länder zu bestimmen und die jährlichen Entwaldungsraten zu berechnen. Diese Studie verwendet NOAA-AVHRR Satellitenbilder in einer Auflösung von 1km x 1km um die Landesfläche von Kontinental-Ecuador in „Wald" bzw. „Nicht-Wald" Pixel zu klassifizieren und die jährliche Entwaldungsrate zwischen 1986 und 2001 sowie zwischen 2001 und 2008 zu bestimmen. The angewandte Methodik basiert auf einem Entscheidungsbaum Algorithmus, der neben verschiedenen Spektralbändern des AVHRR Sensors auch topographische und meteorologische Parameter beinhaltet. Die Ergebnisse zeigen, dass die Waldbedeckung von Kontinental-Ecuador von 48.1 % im Jahr 1986 auf 36.8 % im Jahr 2008 reduziert wurde. Die berechneten jährlichen Entwaldungsraten ergaben, dass die Abholzung der Bestände während des letzten Jahrzehnts sogar zugenommen hat. Das am stärksten betroffene Gebiet ist die Küstenregion, aufgrund des erhöhten Bevölkerungsdrucks; gefolgt vom Amazonastiefland, nicht nur wegen der staatlich geförderten Erdöl- und Bergbauindustrie sondern auch aufgrund der unkontrollierten Holzgewinnung. Das Hochland der Anden ist weniger betroffen, da die meisten Regionen schon früher entwaldet wurden, während der Präkolumbianischen Zeit.

Keywords: Remote sensing, NOAA image processing, forest cover, annual deforestation rates, Ecuador

1 Introduction

Tropical forests cover about 7 % of the Earth's surface and are home to millions of species (e.g. Olander et al. 2008), but during the most recent decades big parts of this unique ecosystem got lost because of human activities. The conversion from forest into pasture or agricultural land took place in all tropical countries, but especially in South-America, where highest deforestation rates are observed (FAO 2010a). Deforestation not only has serious impacts on native species, but also on global climate. As Aguiar et al. (2012) mentioned, deforestation in tropical regions is one of the key components of climate change. Burn activities lead to massive emissions of CO_2, CH_4 and other greenhouse gases into the atmosphere (e.g. Poulter et al. 2010; Saatchi et al. 2011; IPCC 2013). One-third of total greenhouse gas emissions are caused by agriculture practices, which also includes indirect emissions from deforestation as well as from land use-changes (Gilbert 2012). The global portion resulting from deforestation is estimated at 20 % (Olander et al. 2008), which is a considerable fraction relative to total global warming.

Global warming leads to an additional pressure on the tropical ecosystems by coercing species into rapid adaptation. With a mean temperature increase of only 1 °C per century, ecological zones

shift poleward up to 160 km (Thuiller 2007) while the altitudinal belts inside mountainous areas are also modified. This results in an increased rate of species extinction, because the time span to acclimatize, especially for highly adapted species, is too short (Thomas et al. 2004).

Besides global warming, deforestation in tropical forest ecosystems also has a direct impact on the regional and local climate. Fries et al. (2009) and Fries et al. (2012) showed in their studies the conversion from forest into pasture leads to higher temperature amplitudes and less water availability for evapotranspiration processes; the water availability decreases due to the increased runoff over deforested areas. Together with the predicted alterations in rainfall distribution and their amounts, the hydrological cycle may be modified, especially in the most affected regions. The hydrological cycle is fundamental for the primary production of an ecosystem, because the water cycle provides the main ecosystem services (e.g. nutrient availability; Breuer et al. 2013). The expectable modifications in local climate and the water cycle do not only affect species composition and reforestation efforts, but also endanger the water supply for the local population.

Therefore, knowledge about the spatial forest distribution and the human impact on ecosystems are crucial requirements for quantifying biosphere sinks and atmospheric sources of greenhouse gases (DeFries et al. 2000). With countrywide vegetation maps, the stocks and emissions of greenhouse gases can be determined and the most affected areas can be depicted at a local and regional scale (e.g. Tan et al. 2007; Moraes et al. 2013).

The highest deforestation rates in South America are reported for Ecuador (FAO 2010a,b). Thereby, not only the tropical lowland forest is affected, but also the tropical mountain forest (Mosandl et al. 2008). This is especially critical in the Ecuadorian Andes, a global hot spot in biodiversity, where an exceptional abundance of endemic species is located (e.g. Barthlott et al. 2007; Beck et al. 2008; Brehm et al. 2008). The Ecuadorian tropical mountain forest is reduced by slash-and burn activities, due to the growing population and economic incentives as well as the tropical lowland forest in the Amazon Basin, because of the governmental supported oil and mining industry (e.g. Ochoa et al. 2015).

Unfortunately, Ecuador does not have operational surveillance systems to monitor ongoing deforestation. Existing observations are scarce, especially for remote areas, including tropical mountain forest, paramos, and the tropical lowland forest in the Amazon Basin (FAO 2010a). The available datasets are mainly estimates based on statistical models and extrapolations of point observations. As the FAO report (2010b) specifies, the forest cover as well as the annual deforestation rates for Ecuador during the time periods 1990–2000, 2000–2005 and 2005–2010 were calculated by means of regression analyses and projections methods, because of the deficient data availability.

For a reliable quantification of forest cover and its reduction over time, satellite data supply a fast and efficient tool, especially for remote areas (e.g. Yoshikawa and Sanga-Ngoie 2011). Satellite data is widely used for vegetation classifications at a global, continental and local scale. Global vegetation estimations are published in Eastman et al. (2013), using NOAA-AVHRR data (National Oceanic and Atmospheric Administration – Advanced Very High Resolution Radiometer). Another, more recent application is the Global Forest Watch initiative, which generated worldwide forest cover maps based on Landsat satellite data (Global Forest Watch, 2015). For continental South-America, Latifovic et al. (2005) and Yoshikawa and Sanga-Ngoie (2011) also presented vegetation and forest cover maps using NOAA-AVHRR data. At a local scale Göttlicher et al. (2009) published a vegetation classification for southern Ecuador by means of Landsat satellite data.

On a continental to global scale, NOAA-AVHRR satellite data have been widely used to monitor and classify vegetation cover and dynamics (e.g. Zhang et al. 2003; Latifovic et al. 2005; Fuller 2006; Eastman et al. 2013), because this satellite series provides the longest and most comprehensive source of remotely sensed data (Wang et al. 2014). To classify the vegetation cover, composites of the different spectral bands of the NOAA-AVHRR sensor are used to calculate the NDVI (Normalized Difference Vegetation Index) and other derived parameters and metrics (e.g. Loveland et al. 2000; Yoshikawa and Sanga-Ngoie 2011).

Previous studies in South America applied Principal Component Analysis (PCA) for forest classification in specific regions (e.g. Amazon Basin; Nonomura et al. 2003; Yoshikawa and Sanga-Ngoie 2011). However, there are still systematic errors inside the NOAA-AVHRR data used, because the degradation of the spectral images over the life time of the satellite is often not taken into account adequately (Latifovic et al. 2012). Furthermore, forest can only be classified at cloud free pixels within the satellite images (e.g. Wang et al. 2014), which is

especially problematic in Ecuador. As Bendix et al. (2004) and Bendix et al. (2006) showed, the relative annual cloud frequency over some specific areas in Ecuador is frequently higher than 90 %.

Hence, the objective of the present paper is to create forest cover maps for continental Ecuador at a national scale, wherefore the established correction algorithms are adapted to the local conditions. By means of these maps, the annual deforestation rates for the periods 1986 to 2001 and 2001 to 2008 are calculated. This product will be helpful as a baseline for initiatives such us REDD (Reducing Emissions from Deforestation and Forest Degradation), which was implemented by the Ecuadorian Environmental Ministry (MAE – Ministerio del Ambiente) in 2008 (MAE 2015).

To reach these targets, a combination of different methods is applied: First NOAA-AVHRR images are corrected by radiometric adjustments, using the optimized coefficients published by Latifovic et al. (2012). Then geometric rectification of the images is processed, applying orbital satellite parameters and "Image Matching" with ancillary data (Eugenio and Marquez 2003) derived from Landsat satellite images. Finally, to overcome the high cloudiness and cloud contour effects in the satellite image, a combination of the cloud classification and images composition is executed. The final forest classification is based on a decision tree method adapted from Hansen et al. (2000), which additionally includes topographic and climatic parameters.

The paper is structured as follows: In section 2 the study area and the data are presented. Section 3 explains the used methods of the instant forest classification and the calculation of the annual deforestation rates per period. In section 4 the results are presented, discussed and validated. The paper ends with general conclusions.

2 Study area and data

The study has been executed in Ecuador, bordering on Colombia in the north, on Peru in the south and east and by the Pacific Ocean to the west (~1°N to 5°S; ~75°W to 81°W). The altitude ranges from sea-level up to over 6000 m at the highest Andean mountain peaks. The Andes cross the country from the north to the south, wherefore the country can be divided into three principal climatic regions: the Coastal Lowland in the west, the Andean Highland in the centre (Sierra) and the Amazon Basin in the east (Fig.1).

The natural vegetation in Ecuador is determined by these three principal climatic regions. The Coastal Lowland is characterized by semi-deciduous, deciduous forests and savannas; the Amazon Basin by tropical rain forest. The Andean Highland contains altitudinal vegetation belts (Bendix et al. 2008), which can be classified in montane broad-leaved forest and the upper montane forests (Elfin forest), otherwise known as the Ceja Andina. These two forest types are well developed on the eastern escarpment of the Andes and in the northern parts of the western Cordillera. Further to the south at the coastal Cordillera these forest types become more isolated, due to the drier climate conditions and Dry-Forest vegetation and savannas prevail (Diertl 2010). At higher elevations in the northern and central parts grass-páramo vegetation is formed, while shrub-páramo vegetation dominates in the southern part. This difference is caused by the Andean Depression situated between southern Ecuador and northern Peru (Richter 2003), leading to different climatic conditions. The upper treeline in the northern and central parts is situated at ~4000 m asl, determined by the temperature and moisture content of the air; at the southern part the treeline is notably lower (2700 m–3300 m asl), probably caused by the stronger wind conditions (Beck et al. 2008). Nevertheless, biodiversity is extraordinarily high in the area of the Andean Depression, due to the lower top altitudes, which facilitate the exchange between the coastal and the Amazonian vegetation (e.g. Myers et al. 2000; Barthlott et al. 2005; Homeier et al. 2008).

As mentioned above, deforestation rates are highest in Ecuador compared to the other countries in South America (Mosandl et al. 2008; FAO 2010a). Wunder (2000) assumed that the surface of Ecuador was originally covered with forest by 90 % (~25 million ha). This is also confirmed by Cabarle et al. (1989), who estimated an original forest cover of about 26 million ha. There are two main deforestation periods in Ecuador: First a long-lasting deforestation in the Andean Highland over 1200 m asl during the Pre-Colombian-Era and second a fast forest reduction in the Coastal Lowland during the last century (Mosandl et al. 2008). The Coastal Lowland forest was replaced by agricultural crops during the cacao-boom (1900–1920) and the banana-boom (1950–1965; Cabarle et al. 1989). The reduction of the Amazonian rain forest took place in the 1970s, caused by the oil-boom. Until 1990 the total forest cover of continental Ecuador was reduced to 48.7 % and for 2010 a forest cover of about 34.7 % was calculated (~9.9 million ha; FAO 2010b). The recent

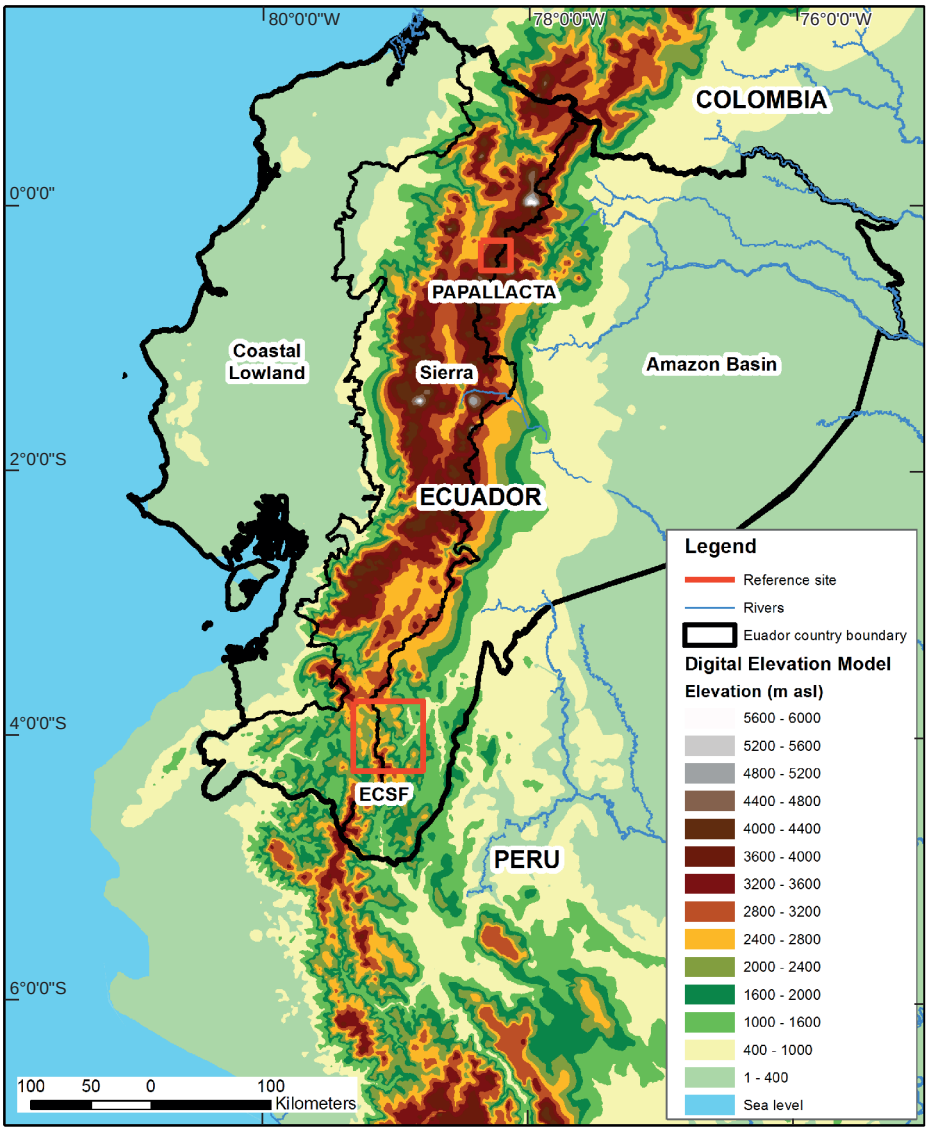

Fig. 1: Digital Elevation Model (DEM; adapted from FARR et al. 2007) of the research area (continental Ecuador), including the three principal regions: Coastal Lowland, Andean Highland and Amazon Basin, as well as the reference sites for validation

deforestation mostly does not affect the primary forest areas, because the majority of these areas are protected. The actual deforestation is mainly observed in secondary forest areas and in the mountain forest ecotones, where nearly the complete forest cover has been replaced by pastures (MOSANDL et al. 2008). Besides the recent land use change from forest to pasture, only small areas of reforestation are recorded for Ecuador compared to other countries in South-America. This additionally amplifies the deforestation rates for Ecuador and leads to the highest values at country level (FAO 2010a).

The Digital Elevation Model (DEM, Fig.1) used in this study was originally created during the Shuttle Radar Topography Mission (SRTM) in 2007 and the data can be freely accessed online (http://www2.jpl.nasa.gov/srtm/southAmerica_sp.htm). The single steps of the DEM generation are published in FARR et al. (2007). For this approach the SRTM data was resampled to 1km x 1km to obtain the same resolution as the NOAA-AVHRR images.

Satellite data for vegetation classification are available from 1970s to present from different satellite types. The spatial resolution of the images

depends on the sensor type installed, ranging from low resolution (4km x 4km; GOES imagery, Simic et al. 2004), over coarse resolution (1 km x 1 km; e.g. NOAA-AVHRR), moderate or medium resolution (up to 250 m x 250 m; e.g. MODIS), high resolution (up to 30 m x 30 m; e.g. Landsat TM), to very high resolution (up to 1 m x 1 m; e.g. Ikonos, QuickBird). In this approach NOAA-AVHRR data is used to classify the forest cover at a national scale, because after a careful inspection of the available data it was found that Landsat TM satellites (operating since the early 1980s) or MODIS (operating since 1999, Chuvieco and Huete 2009), do not cover the geographic boundary of continental Ecuador completely or historical data is not available, which also holds true for newer satellite types as Aster, RapidEye and QuickBird.

The NOAA-AVHRR resolution (1 km x 1 km) is lower compared to MODIS and Landsat TM images, but the data covers the whole continental Ecuador and historical data is available online (NOAA-CLASS 2015; http://www.class.noaa.gov). Furthermore, the coarse resolution of this satellite type fulfill the minimum requirements of the REDD initiative and reforestation programs conducted by MAE (2015), illustrating the forest cover of continental Ecuador in a 1 km x 1 km resolution. The data used here corresponds to the Local Area Coverage (LAC) format. The NOAA-AVHRR sensor provides data of five spectral bands: one in the visible range (channel 1: 0.58-0.68μm), two in the near-infrared range (channel 2: 0.725-1.00μm; channel 3: 1.58-1.64μm (day), 3.55-3.93μm (night)), and two in the thermal infrared range (channel 4: 10.30-11.30μm; channel 5: 11.50-12.50μm). For the forest classification in the present study, channels 1, 2, and 5 were used.

For the calculation of total forest cover and annual deforestation rates in continental Ecuador over the periods 1986–2001 and 2001–2008 a set of NOAA-AVHRR satellite images of the years 1986, 2001 and 2008 are used. 1986 was selected as the base year because reference site data is available to validate the results (Papallacta, Bendix and Rafiqpoor 2001; Fig. 1). Furthermore, total forest cover was estimated by Cabarle et al. (1989), respective to the years 1987/1988, which can be used as reference value. The same is valid for the year 2001 where reference site data is available, too (Estación Científica San Francisco – ECSF, Göttlicher et al. 2009; Fig. 1), and a comparison to the official estimates presented in reports from MAE (2011 and 2012a) and FAO (2010b), respective to the year 2000, can be drawn. The raw data sets of 1986 and 2001 were downloaded from the NOAA-CLASS webpage (Comprehensive Large Array-data Stewardship System). The year 2008 was chosen because the REDD program in Ecuador started in 2008 (MAE 2015) and the calculated forest cover map provide basic data for this initiative. The raw data for the year 2008 was captured by the NOAA-AVHRR receiver station (coordinates: 3.986784 S, 79.198585 W) installed inside the campus of the Technical University of Loja/Ecuador (Universidad Técnica Particular de Loja, UTPL). The station, which consists of an antenna and a signal processor from Quorum Communications (2015), worked from 2007 to 2009 and raw data from all operating satellites could be received directly during this period. The receiver station location permitted a reception of the raw imagines in excellent satellite angles for vegetation classification at least two times a day. As Tucker et al. (2005) explained in their study, vegetation classification based on satellite images only is feasible if the viewing angle of the satellite is lower than 30°, because greater angles cause geometric distortions and blurring of pixels up to 2.4 km x 6 km.

3 Methods

To avoid miscalculations in the applied forest classification method, years with pronounced phenomena like ENSO or droughts, which cause short term variations in regional vegetation cover (under – or overestimation of the real forest cover), were not considered in this study. The same is valid for years of big volcanic eruptions (e.g. Mt. Pinatubo eruption in June of 1991), which bias forest classification by means of satellite data, because the dust in the atmosphere causes interference, wherefore the established thresholds for vegetation classification cannot be applied (Gutman et al. 1998).

The processing of the NOAA-AVHRR images to generate a forest classification for continental Ecuador can be divided in three parts (Fig. 2).

The first step is the correction and calibration of the individual satellite raw images, including systematic corrections, geo-referencing, and cloud elimination. The radiometric corrections eliminate the atmospheric and solar radiation errors in the images (Roderick et al. 1996), whereas specific parameters, suggested by Latifovic et al. (2012), are used. Then, the geometric correction is applied, implicating orbital parameters of each individual NOAA satellite, which are available online at the NOAA Class website, provided by the Advanced Earth Location Data System (EALDS). Next, a geo-referencing process is executed. A detailed description of the single

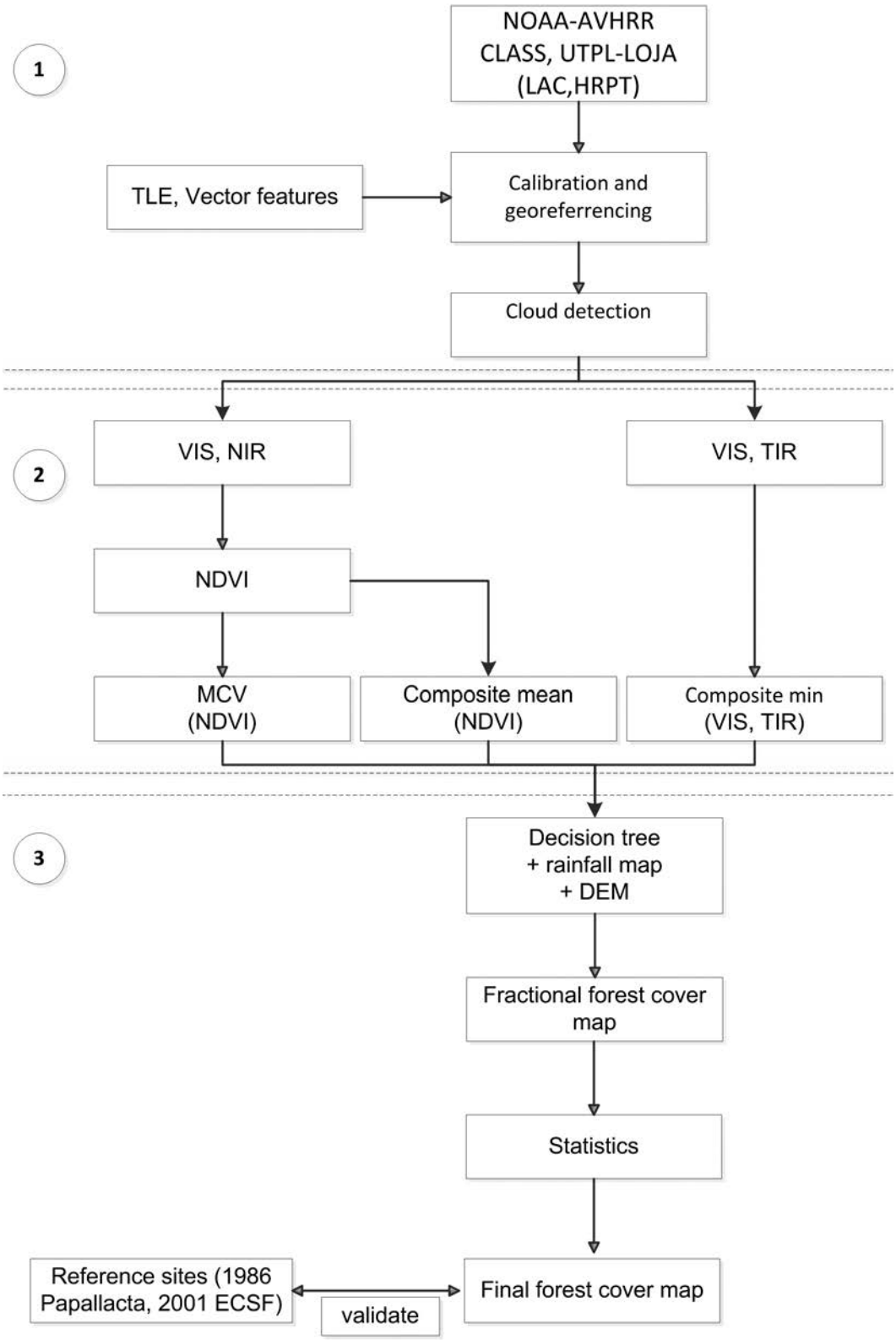

Fig. 2: Processing scheme of the "forest" – "non-forest" classification

steps can be found in Bachmann and Bendix (1992). During the geo-referencing process offsets from 4 km to 6 km frequently occur; hence, an additional adjustment has to be done. This further process is called "Image Matching" (e.g. Eugenio and Marquez 2003; Marcal and Borges 2003; Latifovic et al. 2005) and consists of auxiliary data from vector files, which distinguish and compare specific locations of main geographic features. The vector layer was generated by means of photointerpretation of Landsat Images in MrSID format from 1990 and 2000. The two vector layers compare the recognizable geographic features, such as the coast line, rivers, lakes, glaciers and/or city boundaries of the corrected NOAA images. If the position of these features is incorrect, each individual NOAA image is moved until it matches perfectly with the vector layers.

Hansen et al. (2002) exposed that special attention must be given to areas with clouds and cloud shadows because they alter the spectral values of the affected pixels as well as the pixels around these areas. As stated before, in Ecuador extremely high cloud frequency is present during the whole year (e.g. Bendix et al. 2006), which complicates any kind of satellite image product generation, especially at the escarpments of both cordilleras and at the Costal Lowland in the north (Fig. 3a). The cloud detection scheme to eliminate the affected pixels is adopted from Bendix et al. (2004), which do not only determine cloud-filled pixels, but also classify the general cloud types (Fig. 3b). For further information about the cloud classification please refer to Bendix et al. (2004). The result is a classified cloud mask, which is subtracted from the NOAA image. To avoid errors due to the cloud contour effect and cloud shadows a buffer of two pixels (=2 km) around each cloud field is also eliminated. Additionally, cloud shadows are identified by means of the solar angle and position during the satellite flyover and the affected areas subtracted. The result is a corrected and geo-referenced NOAA image, where all cloud contaminated pixels and shadows are removed.

The second step is the determination of the NDVI for all corrected NOAA images individually. The NDVI index is related to the photosynthetic capacity and hence to the energy absorption of the vegetation and is calculated as the ratio of channels 1 (VIS) and 2 (NIR) of the NOAA-AVHRR sensor (Fensholt et al. 2009):

$$NDVI = \frac{NIR - VIS}{NIR + VIS} \qquad (1)$$

where NIR is the second NOAA-AVHRR channel (0.725-1.00μm) and VIS is the first NOAA-AVHRR channel (0.58-0.68μm).

To fill the cloud gaps in the individual NDVI maps a composite of several images has to be generated, using the Maximum Value Composite (MVC) method. The MVC consists of a multi-temporal com-

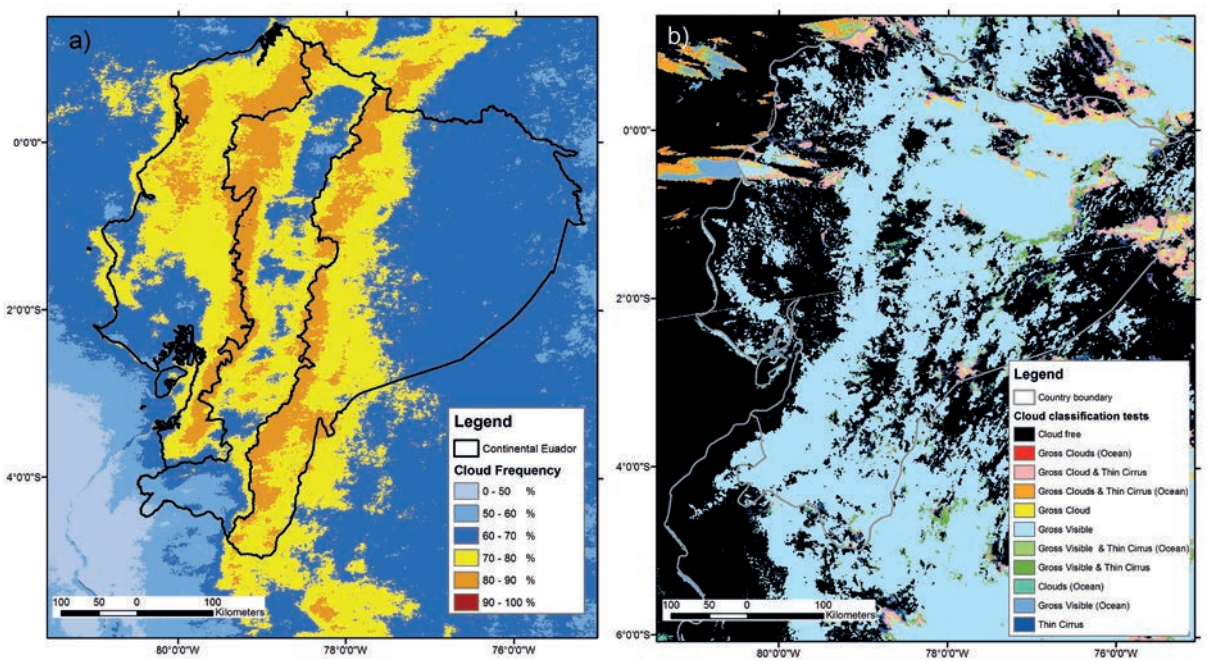

Fig. 3: a) Annual cloud cover map of Ecuador (modified from Bendix et al. 2004); b) Example of a cloud classification map

posite of NDVI maps, where the maximum value for each pixel over a required time span is determined (Chen et al. 2003; Maisongrande et al. 2004). The MVC method also removes remaining clouds in the images, because clouds attenuate the spectral sensor values (Hansen et al. 2002). Generally, a temporal MVC composite of 10-days is created, but due to the high cloud frequency in Ecuador the temporal time span had to be extended to one month (e.g. Loveland et al. 2000; Los et al. 2002; Ma and Veroustraete 2006; Wang et al. 2014). Finally, all monthly composites are merged to annual NDVI maps for the years 1986, 2001 and 2008. However, even in the annual composites blank pixels remain, because in the images of the selected years clouds were always present over some areas, especially at the escarpments of the cordilleras and over the northern Costal Lowland. An example of an annual NDVI composition (year 2001) is shown in figure 4.

Besides the MVC composites of the maximum NVDI maps, composites of the NOAA-AVHRR channels 1 and 5 are generated. These composition products are necessary for the decision tree to obtain the final forest classification (Fig. 5). For channel 5 a composite of maximum values and for channel 1 a composite of minimum values are merged, in the same manner as explained before, and additionally a yearly composite of the mean values of the NDVI is generated.

The third step is the application of a decision tree to classify pixels with or without forest cover. Decision tree algorithms are widely used in forest classifications; because they represent a high overall accuracy (up to 90 %; Lim et al. 1998; Hansen et al.

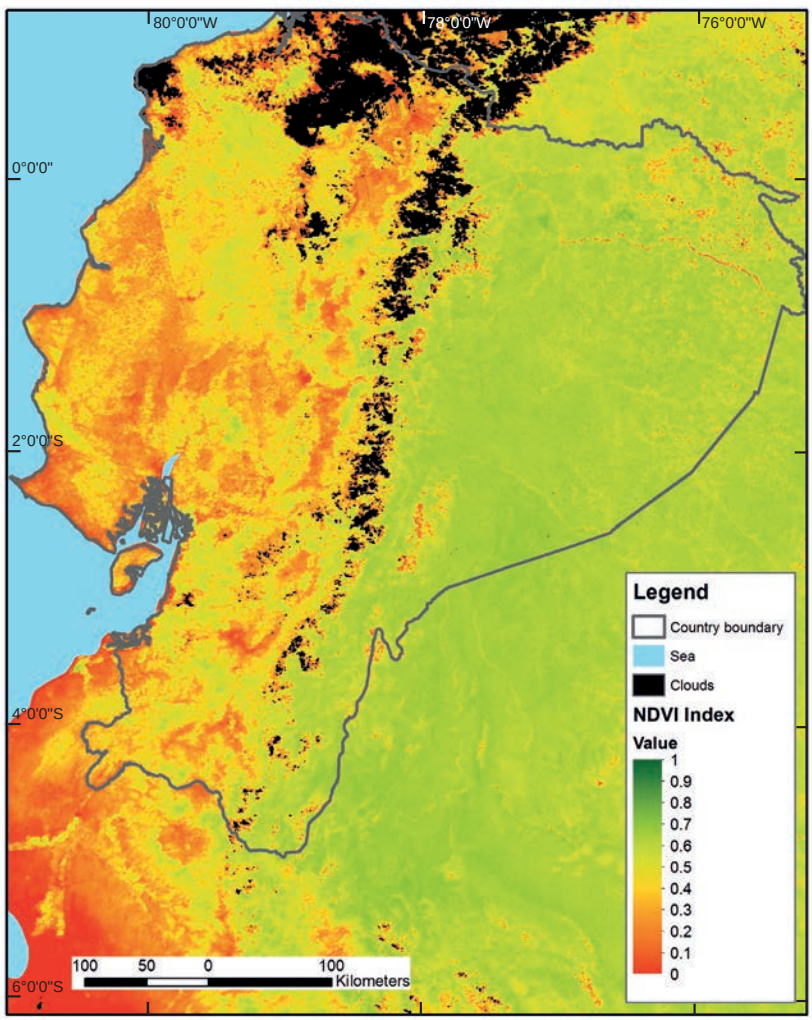

Fig. 4: MVC composite of the annual NDVI (year 2001) with remaining clouds (black color)

2000) and improve discriminations between different vegetation classes especially at coarse resolution (McIver and Friedl 2002). The decision tree algorithm (Fig. 5) is adapted from Hansen et al. (2000) and automatized using the programming language "Fortran". In contrast to the original algorithm, where all five spectral bands of the NOAA-AVHRR sensor were used to classify different forest types, here only the composites of NDVI, channel 1 (VIS) and 5 (TIR) were included to detect "forest" respectively "non-forest" pixels. To improve the forest classification and to avoid false classification, additional topographic and meteorological data (precipitation and altitude) are also integrated in the decision tree algorithm (Fig. 5).

First an annual precipitation threshold was established, because forest vegetation needs at least 300 mm of rainfall per year (Furley 2007). The annual precipitation map was obtained from the WorldClim database (Hijmans et al. 2005; http://www.worldclim.org), which has the same resolution as the NOAA images (1 km x 1 km). Each pixel within the satellite images is compared to the mean annual precipitation value in the WorldClim map (50 years average) and classified as "non-forest" if the threshold is not reached. Then, the remaining pixels are compared to the DEM (Fig. 1), obtained from the SRTM (Farr et al. 2007), which was resampled to the satellite image resolution. Polylepis forest in the tropical Andes can be found in altitudes between 3600 m and ~4200 m (Cierjacks 2007), wherefore the tree-line threshold was set to 4200 m asl and all pixels with higher elevation are flagged as "non-forest". After this, the created composites of VIS, TIR and the NDVI are included in the decision tree (Fig. 6). The respective thresholds of each single step are taken from Hansen et al. (2000). The result is a forest cover map classified into "forest" and "non-forest" pixels for the years 1986, 2001 and 2008.

By means of the generated forest cover map the annual deforestation rates for the time span 1986 to 2001 and 2001 to 2008 are calculated. The annual rate of change can be estimated by comparing the forest cover in the same regions at two different times. According to Puyravaud (2003), the equation can be written as follows:

$$q = \left(\frac{A_2}{A_1} \right)^{1/(t_2 - t_1)} - 1 \qquad (2)$$

where: A_1 y A_2 are the forest cover maps and t_1 and t_2 are the different time periods.

To avoid miscalculations of the annual deforestation rates per period (1986–2001; 2001–2008) the cloud contaminated pixels of both maps had to be merged (1986/2001; 2001/2008 respectively), because clouds cover different areas within each map. Then the merged cloud map is subtracted from both yearly forest classifications to guarantee the comparison of the same regions in the individual maps. Thereby, only pixels which could be classified within both years are taken into account for the calculation of the annual deforestation rate per period.

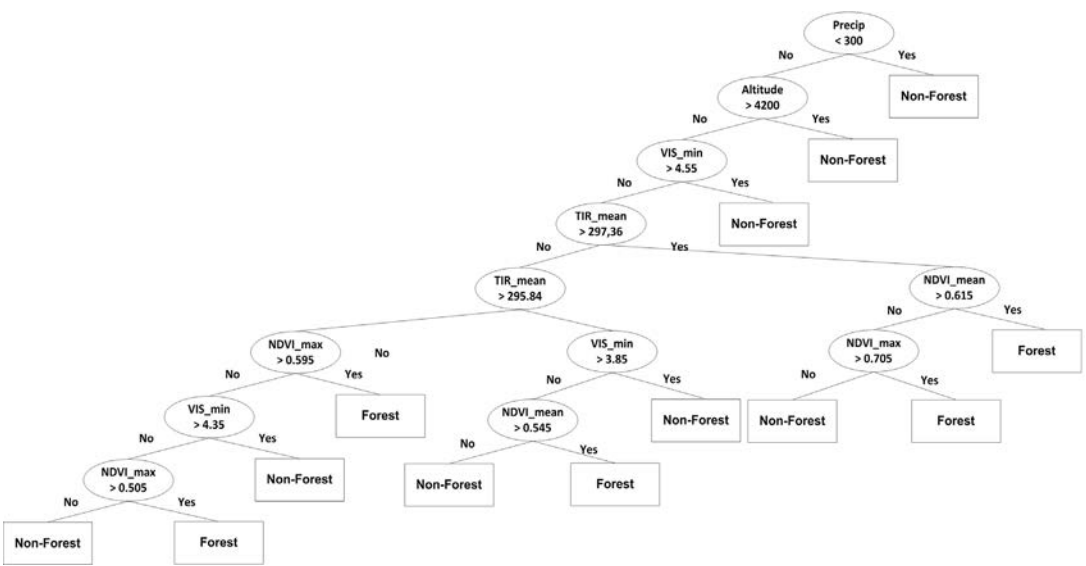

Fig. 5: Decision tree algorithm of the "forest" – "non-forest" classification

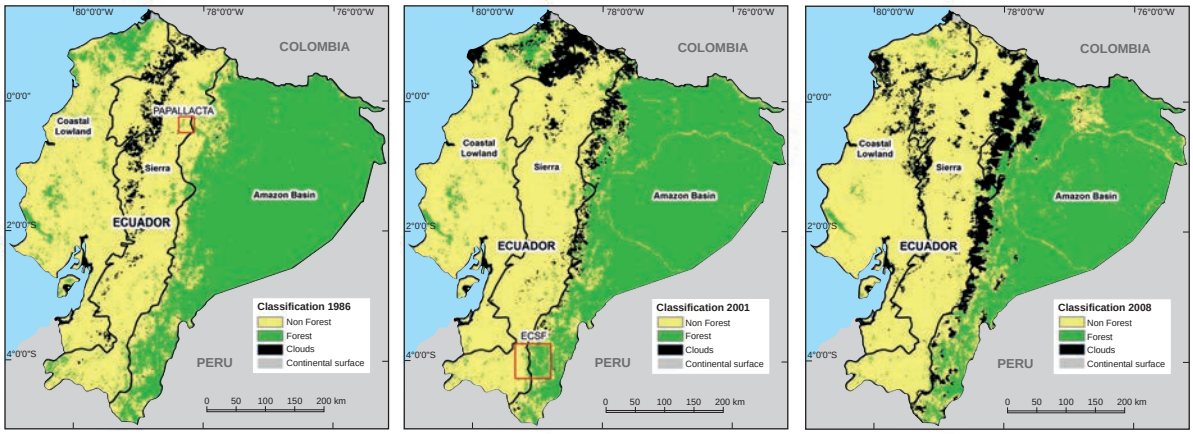

Fig. 6: Forest classification of the year a) 1986 (with reference site), b) 2001 (with reference site) and c) 2008

Finally, to validate the results available ancillary data (reference sites) from 1986 and 2001 are used to compare the generated forest cover map at the respective locations. The land cover at the reference site Papallacta (see Fig. 1; year 1986) was classified using aerial photography by BENDIX and RAFIQPOOR (2001); the reference site ECSF (see Fig. 1; year 2001) by GÖTTLICHER et al. (2009) by means of Landsat satellite images. The reference site vegetation maps are taken as reliable for the respective year, because of the higher resolution of these data. Due to the different resolutions of the aerial photographs, the Landsat classification and NOAA-AVHRR satellite images, a reclassification was necessary. The original pixels with a resolution of 25 m (aerial photography and Landsat) were aggregated into pixels of 1km (NOAA-AVHRR resolution). Then the percentage of forest cover of each aggregated pixel was calculated and declared as "forest" if more than 60 % (threshold) are covered by forest stands (DEFRIES et al. 2000). By comparing the forest cover at the reference sites to the same areas in the generated yearly maps, the accuracy of our results is determined.

4 Results and discussion

The high cloud frequency over continental Ecuador during the whole year (BENDIX et al. 2004) did not permit the creation of cloud free composites to calculate exactly the total forest cover and the annual deforestation rates per decade within the country. The generated forest cover maps always show areas of cloudiness (black color; see Fig. 6a,b,c), therefore a definitive percentage of national forest cover could not be established. In the worst case clouds cover approximately 8.9 % of the continental surface of Ecuador (year 2008; Fig. 6c), which may increase the maximum inaccuracy of the generated maps and the error within the calculation of the annual deforestation rates. However, the final errors are not that pronounced, because clouded pixels mainly occur over areas where only small patches of possible forest can be expected (escarpments of the two cordilleras; see Fig. 6), because most of these areas were previously deforested or the altitudinal threshold is exceeded (CIERJACKS 2007; MOSANDL et al. 2008).

The forest classification map for the year 1986 (Fig. 6a) displays a total forest cover for continental Ecuador of ~11.9 million ha, which is equivalent to 48.1 % of the land surface (Tab. 1). The MAE report (2012a) published a value of about 12.9 million ha for the year 1990, using Landsat satellite images; and the FAO report (2010b), respectively to the year 1990, specifies a total forest cover of 13.8 million ha, equivalent to ~51.0 % of the land surface. The higher amount of forested cover (between ~8.6 % (MAE) and ~16.2 % (FAO)) may be caused by cloud contaminated pixel, which are present in our calculated map (2.7 %, more than 0.7 million ha). Supposing that all contaminated pixel are located over forest stands, our value is close to the MAE report (2012a), but this cannot be expected as figure 6a indicates, because clouds occur mostly over the western cordillera where only small patch of mountain forest are located. The high FAO value is uncertain, as the report (2010a) specifies, due to the lack of information for this period and the applied interpolation method. However, CABARLE et al. (1989) also presented estimates of total forest cover for continental Ecuador for the period 1987-1988, indicating values between

43 % and 50 %, with a possible maximum forest cover of 13.6 million ha. The established range confirms our value of total forest cover of continental Ecuador at the end of the 1980s, although in our map cloud contaminated pixels are present.

Figure 6a illustrates that most of the Coastal Lowland and the Andean Highland are deforested, due to the intense deforestation phases during the last century and during the Pre-Colombian-Era (e.g. WUNDER 2000). The Coastal Lowland only show bigger patches of forest in the northern and the central parts, where protected areas were established (e.g. Reserva Ecológica, Manglares, Cayapas Mataje; Reserva Ecóliga, Cotacachi Cayapas; Reserva Ecológica, Mache Chindul; Parque Nacional Machalilla; MAE 2012b). The Andean Highland forest basically covers uninhabited and/or steep valleys, whereas population pressure on the mountain ecosystems was still low during this period. In the extreme south, isolated patches of forest can be seen as well, indicating intact Dry Forest (west) and Tropical Mountain Forest (east) stands near the border of Peru. The Amazon Basin shows nearly a complete forest cover, except for the regions at the escarpment of the eastern cordillera and bigger areas in the southeast. These areas were deforested during the oil-boom, especially the northern and central parts, and with the beginning of the big scale mining industry in the southern part, during the 1970s (BONAN 2008). Inside the forest, along the big river systems, "non-forest" pixels are displayed, too, which is not only caused by the timber extraction, but also due to the existing water surfaces (see Fig. 1).

Figure 6b shows the forest classification for the year 2001. Forest covers 10.4 million ha (~42.0 %, Tab. 1)) of continental Ecuador. The MAE report (2012a) specifies a value of 11.8 million ha for the year 2000, the same value is reported by the FAO (2010b). These results, compared to our study, indicate a higher forest cover of continental Ecuador of about 1.6 million ha (~13.5 %). This may be due to the high number of cloud affected pixels in our generated forest cover map (5.3 %, more than 1.3 million ha; Tab.1). However, an earlier MAE report (2011) specifies lower values of total forest cover in continental Ecuador between 10.5 million ha (MAE) and 11.6 million ha (CLIRSEN = Centro de Levantamientos Integrados de Recursos Naturales por Sensores Remotos del Ecuador) for the year 2000.

Tab. 1: Results of the comparison between reference sites and the new classification approach. The mean values show the percentage of forest present in class of forest/non-forest

Year	Land cover	Total land surface [ha]	Forest cover [%]	Cloud cover [%]	Forest cover reduction in relation to 1986 [%]	Annual rates of deforestation [%]
1986	Non Forest	12132500				
	Forest	11871700	48.1		0.0	
	Clouds	654800		2.7		
	Total Area	24659000				
						1986–2001
2001	Non Forest	12975600				
	Forest	10368500	42.0		12.7	-0.9
	Clouds	1314900		5.3		
	Total Area	24659000				
						2001–2008
2008	Non Forest	13393800				
	Forest	9062800	36.8		23.7	-1.9
	Clouds	2202400		8.9		
	Total Area	24659000				

Compared to the year 1986 (Fig. 6a) a reduction in forest cover of 12.7 % could be stated (see Tab. 1). Forested areas were considerably reduced in the whole country during the end of the last century, but especially at the Coastal Lowland and in the Andean Highland (see: Supplement), where forest was replaced by pastures and agricultural land (e.g. Mosandl et al. 2008). At the Costal Lowland deforestation took place even in the protected areas to the north and the central parts, only the core areas still show bigger patches of connected forests. Big parts of the Dry Forest in the south of the Andean Highland as well as most of the Tropical Mountain Forest in the Andean valleys got lost, too, due to the enhanced population pressure (Ochoa et al. 2015). The Amazonian Basin also displays an increase of deforested areas, especially in the south-east near the border with Peru, mainly caused by the intense mining industry. Along the streams a reduction is visible, too, which is due to uncontrolled timber extraction near the bigger rivers.

The calculated annual deforestation rate for the period 1986 to 2001 is ~-0.9 % (Tab. 1), considering only areas which could be classified at both years (subtraction of the merged cloud mask). The FAO (2010a,b) published a notably higher deforestation rate for the period 1990–2000 (-1.5 %). The difference may be caused by the high amount of cloud covered pixels in our map, especially over the northern Costal Lowland. However, as explained above the published deforestation rate for Ecuador in the FAO reports (2010a,b) for the decade 1990 to 2000 is uncertain and MAE (2012a) indicates a value of -0.7 % for the same period.

Figure 6c displays the forest classification map for 2008. Forest covers 9.1 million ha of the land surface, which compared to the year 1986 is a reduction in forest cover of 23.7 % (Tab. 1) and to the year 2001 of 12.6 %. The FAO reports (2010b) specify a total forest cover for continental Ecuador of ~9.9 million ha for the year 2010, which means a reduction of 28.3 % compared to the year 1990. In contrast, MAE (2012a) published a value of 11.3 million ha for the year 2008. Again, the difference in forest cover may be due to the high number of clouded pixels in our map (8.9 %, more than 2.2 million ha; Tab. 1).

Deforestation continued during the last decade in the whole country not only at the Coastal Lowland and the Andean Highland, but also in the Amazon Basin (Fig. 6c). At the Coastal Lowland most of the forest stands are cleared to create agricultural land, due to the enhanced population pressure. Only in the core parts of major protected areas patches of dense forest still remain. The same scenario can be observed in the Andean Highland, where the forest is almost replaced completely to create pasture land (e.g. Mosandl et al. 2008; Ochoa et al. 2015). The most obvious reduction of forest cover is displayed in the north of the Amazon Basin, where oil companies expanded their production, while the expansion of the mining industry took place in the southeast (see: Supplement). Furthermore, small patches of several deforested areas inside the Tropical Lowland Forest are visible, which is mainly caused by illegal timber extraction (Bonan 2008). But now, the clearance of the forest is not only shown near the bigger river systems but also in parts of difficult accessibility.

The calculated annual deforestation rate is -1.9 % (Tab. 1), respectively to the period 2001 to 2008. FAO (2010b) specifies the same value, while the MAE report (2012a) a notable lower value of -0.7 %. The low annual deforestation rate published by MAE (2012a) seems to be underestimated, because other studies also confirm the increase of the deforestation rate in continental Ecuador during the last decade (e.g. Mosandl et al. 2008; Tapia et al. 2015).

The forest classification of continental Ecuador was validated be means of the generated maps for 1986 and 2001, and data from two independent study sites. For 1986 a photointerpretation product for a small area in northern Ecuador (Papallacta at 4800 m asl; Bendix and Rafiqpoor 2001; Fig. 7) is available and for 2001 a Landsat TM classification for an area in southern Ecuador (ECSF at 1850 m asl; Göttlicher et al. 2009; Fig. 8). First, both independent data sets were resampled to the same spatial resolution as the NOAA-AVHRR images (1 km x 1 km) and reclassified in "forest" and "non-forest" pixels. To classify a pixel as "forest" at least 60 % of it must be covered by forest stands (threshold; DeFries et al. 2000). Then, the respective areas in our maps were subtracted and finally, the areas compared using the "Cross-Tabulation" application in the Idrisi-Taiga software package (IDRISI 2011; Clark Labs 2015). For the year 2001 additionally a cloud mask was generated, because the composite shows some cloud contaminated pixels within the reference site. The cloud mask was subtracted from both maps (reference site and composite) to ensure the comparison of the same areas (see Fig. 8)

The validation for the composite of 1986 (Fig. 7) produced a good accuracy with a Cramer's value of 0.704 and an overall Kappa value of 0.702 (see Tab. 2). The discrepancies may be explained by the

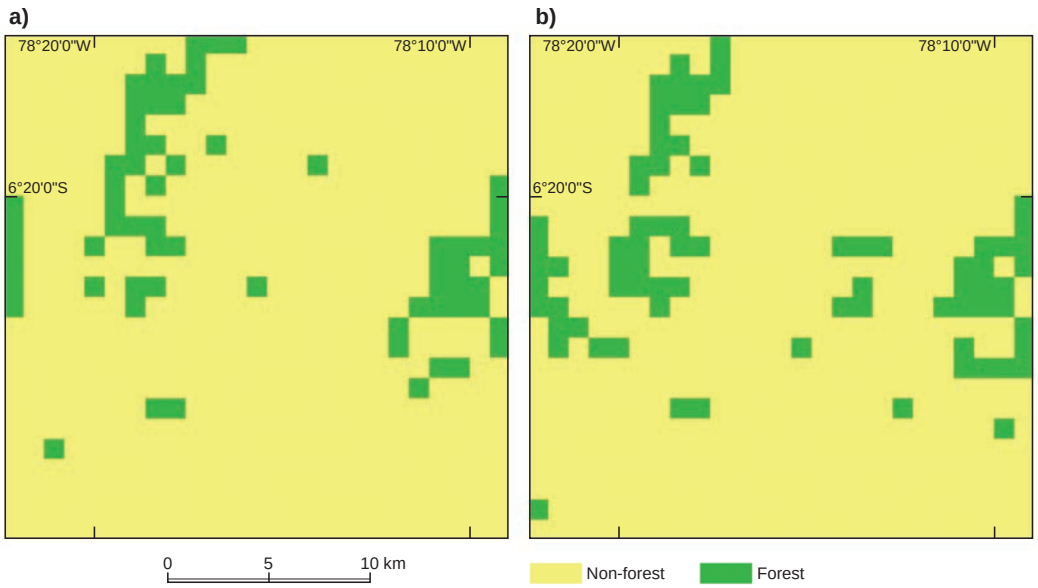

Fig. 7: Forest classification at Papallacta for 1986 a) Reference site (adapted from BENDIX and RAFIQPOOR 2001), b) Classified NOAA-AVHRR image

resampling technique applied to the photointerpretation map of 1986, the established forest threshold (60 %) and/or the different classification methods. However, HANSEN et al. (2000) obtained a similar agreement between 65 % and 82 % for their forest classification map, compared to different training sites. Also MAE (2012a) specified an equivalent overall Kappa value of about 0.7 for their classification, using Landsat satellite images.

Also for the composite of 2001 (Fig. 8) a good accuracy was obtained with a Cramer value of 0.730 and an overall Kappa value of 0.720 (see Tab. 2). The MAE report (2012a) stated the same accuracy for the year 2000 as for the year 1990 (overall Kappa 0.7) for their classification. Unfortunately, the FAO report (2010b) does not specify the accuracy of their maps; it only indicates that the errors are higher for 1990 due to the poor information compared to the year 2010.

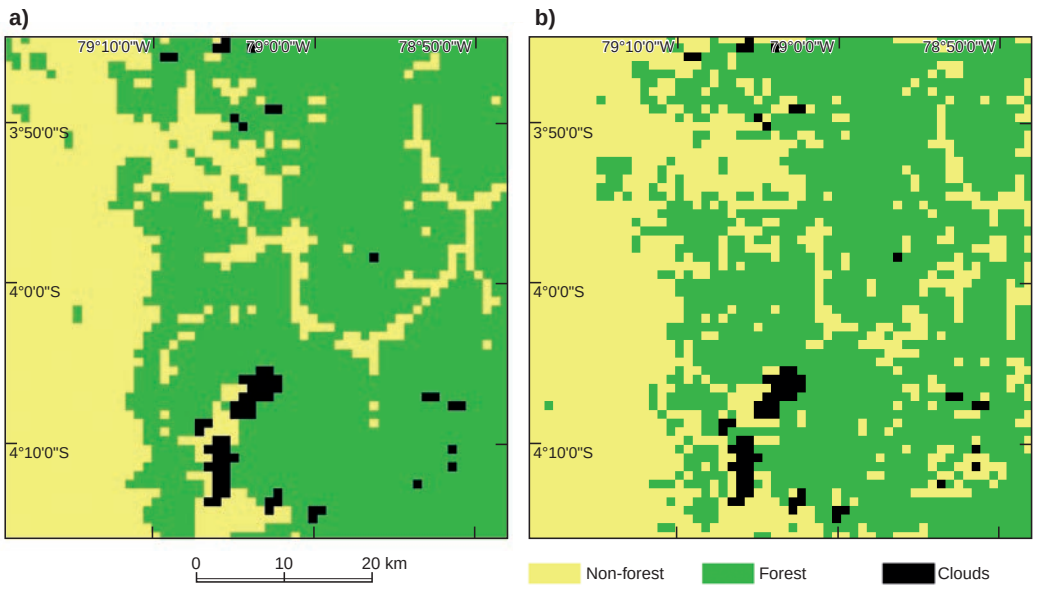

Fig. 8: Forest Classification at ECSF for 2001 a) Reference site (adapted from GÖTTLICHER et al. 2009), b) Classified NOAA-AVHRR image

Tab. 2: Accuracy between "forest" and "non-forest" pixel of the reference sites (rows); a) Papallacta 1986; b) ECSF 2001) and the generated forest cover maps (columns)

Cramer's value		Non-forest	Forest	Total	User's Accuracy	Commission's error
Papallacta	**Non-Forest**	0.8544	0.0384	0.8928	95.69	4.31
	Forest	0.0224	0.0848	0.1072	79.1	20.9
	Total	0.08768	0.1232	1		
	Producer's Accuracy	97.44	68.83			
	Omision's error	2.56	31.67			
Overall Accuracy	**0.9392**					
Cramer's value	**0.7041**					
Overall Kappa	**0.7019**					

b		Non-forest	Forest	Total	User's Accuracy	Commission's error
Loja	**Non-Forest**	0.3513	0.0291	0.3805	92.34	7.66
	Forest	0.108	0.5115	0.6195	82.56	17.44
	Total	0.4593	0.5407	1		
	Producer's Accuracy	76.48	94.61			
	Omision's error	23.52	5.39			
Overall Accuracy	**0.8628**					
Cramer's value	**0.7298**					
Overall Kappa	**0.7203**					

5 Conclusions

The methodology used for forest classification of continental Ecuador, including cloud detection and subtraction, the generation of the annual composites and the application of a decision tree algorithm provides a practical approach to estimate forest cover at a national scale. Compared to other studies and methods the accuracies of the generated maps were determined to be within the same range (FAO 2010b; MAE 2012a), which confirms the reliability of the present approach.

The focus of the present investigation was to calculate the total forest cover and annual deforestation rates per period for continental Ecuador. Unfortunately, clouds were always present over some areas during the selected years and an exact percentage of national forest cover could not be established. However, using composites of one year a lot of the clouded pixels could be eliminated and the additional integration of topographic and meteorological parameters (precipitation and altitude) in the decision tree improved the forest classification.

The study has shown that forest cover in continental Ecuador was clearly reduced during the observation period (from 48.1 % in 1986 to 36.8 % in 2008; Tab. 1). A definitive value of existing forest stand could not be established due to the cloud contamination in the individual maps. Nevertheless, the calculated total forest cover is close to the values presented in other studies (Cabarle et al. 1989, year 1986; MAE 2011, year 2001; FAO 2010b, year 2008). Forest reduction is especially obvious in the Costal Lowland where only in the core zones of protected areas dense forest stands still remain. In this region deforestation is mainly caused by

the enhanced population pressure. The Amazon Basin shows a notable reduction in forest cover as well, mostly resulting from the expansion of the oil and mining industry but also from the illegal timber extraction. The Andean forest stands display lesser deforestation, because most of the mountain forest was cleared during the Pre-Columbian-Era (Mosandl et al. 2008). Highest forest reduction can be stated for the eastern cordillera, as confirmed by MAE (2012a), due to the ongoing mining industry (Fig. 6).

It was also found that annual deforestation rates have increased with the beginning of the new century (-0.9 %, period 1986–2001; -1.9 %, period 2001–2008; see Tab. 1), which is confirmed by the FAO report (2010b) and other studies (Mosandl et al. 2008; Tapia et al. 2015). Although a definitive value could not be established due to the cloud contamination in the individual maps and the inaccuracies of the generated composites (Kappa-value: 0.7; Tab. 2), the obtained results are close to MAE (2012a), respective to the period 1990–2000, and the FAO report (2010b), respective to the period 2000–2010.

To promote reforestation, the national government of Ecuador started a restoration program and identified 1.6 million ha of possible forest restoration (MAE 2014). The generated forest cover maps depict the remaining forest stands and can help to expedite the reforestation program. The maps also are important for the REDD initiative driven by the Ecuadorian government since 2008, because forests are important stocks and sinks for carbon and other greenhouse gases.

To improve the results, future works should generate composites of several years to obtain cloud free forest cover maps of continental Ecuador. Also, additional topographic and meteorological parameters (e.g. landslide and temperature maps) can be integrated to avoid false calculations during the classification process. By means of these maps, total forest cover, annual deforestation rates and possible forest restoration area can be detected more adequately.

Acknowledgements

This study was executed in framework with the DFG Research Unit 816: Biodiversity and Sustainable Management of Mega-diverse Mountain Ecosystems in South Ecuador. Thanks to the members of the Laboratory of Climatology and Remote Sensing (LCRS) in Marburg for their support. Special thanks go to the Universidad Técnica Particular de Loja (UTPL) to facilitate this research.

References

Aguiar, A. P. D.; Ometto, J. P.; Nobre, C.; Lapola, D. M.; Almeida, C.; Vieira, I. C.; Soares, J. V.; Alvala, R.; Saatchi, S.; Valeriano, D. and Castilla-Rubio, J. C. (2012): Modeling the spatial and temporal heterogeneity of deforestation-driven carbon emissions: the INPE-EM framework applied to the Brazilian Amazon. In: Global Change Biology 18, 3346–3366. DOI: 10.1111/j.1365-2486.2012.02782.x

Bachmann, M. and Bendix, J. (1992): An improved algorithm for NOAA-AVHRR image referencing. In: International Journal of Remote Sensing 13, 3205–3215. DOI: 10.1080/01431169208904111

Barthlott, W.; Mutke, J.; Rafiqpoor, M. D.; Kier, G. and Kreft, H. (2005): Global centers of vascular plant diversity. In: Nova Acta Leopoldina NF 92, 61–83.

Barthlott, W.; Hostert, A.; Kier, G.; Küper, W.; Kreft, H.; Mutke, J.; Rafiqpoor, M. D. and Sommer, J. H. (2007): Geographic patterns of vascular plant diversity at continental to global scales. In: Erdkunde 61, 305–315. DOI: 10.3112/erdkunde.2007.04.01

Beck, E.; Makeschin, F.; Haubrich, F.; Richter, M.; Bendix, J. and Valarezo, C. (2008): The ecosystem (Reserva Biológica San Francisco). In: Beck, E.; Bendix, J.; Kottke, I.; Makeschin, F. and Mosandl, R. (eds.): Gradients in a tropical mountain ecosystem of Ecuador. Berlin, Heidelberg, 1–13. DOI: 10.1007/978-3-540-73526-7_1

Bendix, J. and Rafiqpoor, M. D. (2001): Studies on the thermal conditions of soils at the upper tree line in the Páramo of Papallacta (Eastern Cordillera of Ecuador). In: Erdkunde 55, 257–276. DOI: 10.3112/erdkunde.2001.03.04

Bendix, J.; Rollenbeck, R. and Palacios, E. (2004): Cloud detection in the Tropics – a suitable tool for climate-ecological studies in the high mountains of Ecuador. In: International Journal of Remote Sensing 25, 4521–4540. DOI: 10.1080/01431160410001709967

Bendix, J.; Rollenbeck, R.; Göttlicher, D. and Cermak, J. (2006): Cloud occurrence and cloud properties in Ecuador. In: Inter-Research Climate Research 30, 133–147. DOI: 10.3354/cr030133

Bendix, J.; Rollenbeck, R.; Richter, M.; Fabian, P. and Emck, P. (2008): Climate. In: Beck, E.; Bendix, J.; Kottke, I.; Makeschin, F. and Mosandl, R. (eds.): Gradients in a tropical mountain ecosystem of Ecuador. Berlin, Heidelberg, 63–73.

Bonan, G. B. (2008): Forests and climate change: Forcings, feedbacks, and the climate benefits of forests. In: Science 320, 1444–1449. DOI: 10.1126/science.1155121

Brehm, G.; Homeier, J.; Fiedler, K.; Kottke, I.; Illig, J.; Nöske, N. M.; Werner, F. a. and Breckle, S.-W. (2008): Mountain rain forests in southern Ecuador as a hotspot of biodiversity – limited knowledge and diverging pat-

terns. In: Beck, E.; Bendix, J.; Kottke, I.; Makeschin, F. and Mosandl, R. (eds.): Gradients in a tropical mountain ecosystem of Ecuador. Berlin, Heidelberg, 15–24. DOI: 10.1007/978-3-540-73526-7_2

Breuer, L.; Windhorst, D.; Fries, A. and Wilcke, W. (2013): Supporting, regulation, and provisioning hydrological services. In: Bendix, J.; Beck, E.; Bräuning, A.; Makeschin, F.; Mosandl, R.; Scheu, S. and Wilcke, W. (eds.): Ecosystem services, biodiversity and environmental change in a tropical mountain ecosystem of south Ecuador. Berlin, Heidelberg, 107–116. DOI: 10.1007/978-3-642-38137-9_9

Clark Labs (2015): Geospatial software for monitoring and modeling the Earth system. http://www.clarklabs.org/ (Date: 25.06.2015)

Cabarle, B. J.; Crespi, M.; Dodson, C. H.; Luzuriaga, C.; Rose, D. and Shores, J. N. (1989): An assessment of biological diversity and tropical forests for Ecuador. USAID, Quito.

Cierjacks, A. (2007): Environmental and human influences on tropical treeline formation: insights from the regeneration ecology of Polylepis spp. in the Páramo de Papallacta, Ecuador. PhD thesis. Halle.

Chuvieco, E. and Huete, A. (2009): Fundamentals of satellite remote sensing. Boca Raton.

Chen, P.-Y.; Srinivasan, R.; Fedosejevs, G. and Kiniry, J.R. (2003): Evaluating different NDVI composite techniques using NOAA-14 AVHRR data. In: International Journal of Remote Sensing 24, 3403–3412. DOI: 10.1080/0143116021000021279

DeFries, R. S.; Hansen, M. C.; Townshend, J. R. G.; Janetos, A. C. and Loveland, T. R. (2000): A new global 1-km dataset of percentage tree cover derived from remote sensing. In: Global Change Biology 6, 247–254. DOI: 10.1046/j.1365-2486.2000.00296.x

Dierti, K.-H. (2010): Pflanzendiversität entlang eines Höhengradienten in den Anden Südecuadors. Erlangen.

Eastman, J. R.; Sangermano, F.; Machado, E. A.; Rogan, J. and Anyamba, A. (2013): Global trends in seasonality of Normalized Difference Vegetation Index (NDVI), 1982–2011. In: Remote Sensing 5, 4799–4818. DOI: 10.3390/rs5104799

Eugenio, F. and Marques, F. (2003): Automatic satellite image georeferencing using a contour-matching approach. In: IEEE Transactions on Geosciences and Remote Sensing 41, 2869–2880. DOI: 10.1109/TGRS.2003.817226

FAO (Food and Agriculture Organization of the United Nations) (2010a): Evaluación de recursos forestales mundiales 2010 – Informe principal. Roma.

– (2010b): Evaluación de los recursos forestales mundiales 2010 – Informe Nacional Ecuador. Roma.

Farr, T. G.; Rosen, P. A.; Caro, E.; Crippen, R.; Duren, R.; Hensley, S.; Kobrick, M.; Paller, M.; Rodriguez, E.; Roth, L.; Seal, D.; Shaffer, S.; Shimada, J.; Umland, J.; Werner, M.; Oskin, M.; Burbank, D. and Alsdorf, D. (2007): The Shuttle Radar Topography Mission. In: Reviews of Geophysics 45. DOI: 10.1029/2005RG000183

Fensholt, R.; Rasmussen, K.; Nielsen, T. T. and Mbow, C. (2009): Evaluation of earth observation based long term vegetation trends – Intercomparing NDVI time series trend analysis consistency of Sahel from AVHRR GIMMS, Terra MODIS and SPOT VGT data. In: Remote Sensing of Environment 113, 1886–1898. DOI: 10.1016/j.rse.2009.04.004

Fries, A.; Rollenbeck, R.; Göttlicher, D.; Nauss, T.; Homeier, J.; Peters, T. and Bendix, J. (2009): Thermal structure of a megadiverse Andean mountain ecosystem in southern Ecuador and its regionalization. In: Erdkunde 63 (4), 321–335. DOI: 10.3112/erdkunde.2009.04.03

Fries, A.; Rollenbeck, R.; Nauss, T.; Peters, T. and Bendix, J. (2012): Near surface air humidity in a megadiverse Andean mountain ecosystem of southern Ecuador and its regionalization. In: Agricultural and Forest Meteorology 152, 17–30. DOI: 10.1016/j.agrformet.2011.08.004

Fuller, D.-O. (2006): Tropical forest monitoring and remote sensing: a new era of transparency in forest governance?. In: Singapore Journal of Tropical Geography 27, 15–29. DOI: 10.1111/j.1467-9493.2006.00237.x

Furley, P. A. (2007): Tropical forest of the lowlands. In: Veblen, T.; YOUNG, K.; Orme, A. (eds.): The physical geography of South America. New York, 135–157.

Gilbert, N. (2012): One third of our greenhouse gas emissions come from agriculture. In: Nature News & Comment. DOI: 10.1038/nature.2012.11708

Global Forest Watch (2015): Global Forest Watch. http://www.globalforestwatch.org/ (Date: 02.10.2015)

Göttlicher, D.; Obregon, A.; Homeier, J.; Rollenbeck, R.; Nauss, T. and Bendix, J. (2009): Land-cover classification in the Andes of southern Ecuador using Landsat ETM+ data as a basic for SVAT modelling. In: International Journal of Remote Sensing 30, 1867–1886. DOI: 10.1080/01431160802541531

Gutman, G.; Tarpley, D.; Ignatov, A. and Olson, S. (1998): Global AVHRR products for land climate studies. In: Advances in Space Research 22, 1591–1594. DOI: 10.1016/S0273-1177(99)00118-0

Hansen, M. C.; DeFries, R. S.; Townshend, J. R. G. and Sohlberg, R. (2000): Global land cover classification at 1 km spatial resolution using a classification tree approach. In: International Journal Remote Sensing 21, 1331–1364. DOI: 10.1080/014311600210209

Hansen, M. C.; DeFries, R. S.; Townshend, J. R. G.; Marufu, L. and Sohlberg, R. (2002): Development of a MODIS tree cover validation data set for Western Province, Zambia. In: Remote Sensing of Environment 83, 320–335. DOI: 10.1016/S0034-4257(02)00080-9

Hijmans, R.; Cameron, S. E.; Parra, J. L.; Jones, P. G. and Jarvis, A. (2005): Very high resolution interpolated climate

surfaces for global land areas. In: International Journal of Climatology 25, 1965–1978. DOI: 10.1002/joc.1276

Homeier, J.; Werner, F. A.; Gradstein, S. R.; Breckle, S. W. and Richter, M. (2008): Potential vegetation and floristic composition of Andean forests in South Ecuador, with a focus on the RBSF. Mountain rain forests in southern Ecuador as a hotspot of biodiversity – limited knowledge and diverging patterns. In: Beck, E.; Bendix, J.; Kottke, I.; Makeschin, F. and Mosandl, R. (eds.): Gradients in a tropical mountain ecosystem of Ecuador. Berlin, Heidelberg, 87–100. DOI: 10.1007/978-3-540-73526-7_10

IDRISI (2011): Manual Version 16. Worcester.

IPCC (Intergovernmental Panel on Climate Change) (2013): Working Group I Contribution to the IPCC fifth assessment report climate change 2013: The Physical Science Basics. Stockholm.

Latifovic, R.; Trishchenko, A. P.; Chen, J.; Park, W. B.; Khlopenkov, K. V.; Fernandes, R.; Pouliot, D.; Ungureanu, C.; Luo, Y.; Wang, S.; Davidson, A. and Cihlar, J. (2005): Generating historical AVHRR 1 km baseline satellite data records over Canada suitable for climate change studies. In: Canadian Journal of Remote Sensing 31, 324–346. DOI: 10.5589/m05-024

Latifovic, R.; Pouliot, D. and Dillabaugh, C. (2012): Identification and correction of systematic error in NOAA AVHRR long-term satellite data record. In: Remote Sensing of Environment 127, 84–97. DOI: 10.1016/j.rse.2012.08.032

Lim, T.; Loh, W. and Shih, Y. (1998): An empirical comparison of decision trees and other classification methods. In: Madison technical report 979. University of Wisconsin.

Los, S. O.; Tucker, C. J.; Anyamba, A.; Cherlet, M.; Collatz, G. J.; Giglio, L.; Hall, F. G. and Kendall, J. A. (2002): The biosphere: a global perspective. In: Skidmore, A. (ed.): Environmental modelling with GIS and remote sensing. London, New York, 70–96. DOI: 10.1201/9780203302217.ch5

Loveland, T.R.; Reed, B. C.; Brown, J. F.; Ohlen, D. O.; Zhu, Z.; Yang, L. and Merchant, J. W. (2000): Development of a global land cover characteristics database and IGBP DISCover from 1 km AVHRR data. In: International Journal of Remote Sensing 21, 1303–1330. DOI: 10.1080/014311600210191

Ma, M. and Veroustraete, F. (2006): Reconstructing pathfinder AVHRR land NDVI time-series data for the Northwest of China. In: Advances in Space Research 37, 835–840. DOI: 10.1016/j.asr.2005.08.037

MAE (Ministerio del Ambiente | Ecuador) (2011): Estimación de la Tasa de Deforestación del Ecuador Continental. Quito. http://simce.ambiente.gob.ec/sites/default/files/documentos/geovanna/Estimaci %C3 %B3n %20de %20 la %20Tasa %20de %20Deforestaci %C3 %B3n %20 del %20Ecuador %20Continental.pdf (Date: 25.06.2015)

– (2012a): Línea base de deforestación del Ecuador Continental. Quito. http://sociobosque.ambiente.gob.ec/files/Folleto %20mapa-parte1.pdf (Date: 25.06.2015)

– (2012b): Sistema Nacional de áreas protegidas del Ecuador. Quito. http://www.ambiente.gob.ec/wp-content/uploads/downloads/2012/10/SNAP_19_09_12.pdf (Date: 25.06.2015)

– (2014): Plan nacional de Restauración Forestal 2014–2017. Quito. http://sociobosque.ambiente.gob.ec/files/images/articulos/archivos/amrPlanRF.pdf (Date: 25.06.2015)

– (2015): Cambio climático una estrategia transversal de desarrollo. Quito. http://www.ambiente.gob.ec/cambio-climatico-una-estrategia-transversal-de-desarrollo/ (Date: 24.06.2015)

Maisongrande, P.; Duchemin, B. and Dedieu, G. (2004): VEGETATION/SPOT: an operational mission for the Earth monitoring; presentation of new standard products. In: International Journal of Remote Sensing 25, 9–14. DOI: 10.1080/0143116031000115265

Marcal, A. R. S. and Borges, J. (2003): AVHRR rectification using orbital navigation and image matching. In: Image and Signal Processing for Remote Sensing VIII, 13–21. DOI: 10.1117/12.463515

McIver, D. K. and Friedl, M. A. (2002): Using prior probabilities in decision-tree classification of remotely sensed data. In: Remote Sensing of Environment 81, 253–261. DOI: 10.1016/S0034-4257(02)00003-2

Moraes, E. C.; Franchito, S. and Rao, B. (2013): Amazonian deforestation: impact of global warming on the energy balance and climate. In: Journal of Applied Meteorology and Climatology 52, 521–530. DOI: 10.1175/JAMC-D-11-0258.1

Mosandl, R.; Günter, S.; Stimm, B. and Weber, M. (2008): Ecuador suffers the highest deforestation rate in South America. In: Beck, E.; Bendix, J.; Kottke, I.; Makeschin, F. and Mosandl, R. (eds.): Gradients in a tropical mountain ecosystem of Ecuador. Berlin, Heidelberg, 37–40. DOI: 10.1007/978-3-540-73526-7_4

Myers, N.; Mittermeier, R. A.; Mittermeier, C. G.; da Fonseca, G. A. B. and Kent, J. (2000): Biodiversity hotspots for conservation priorities. In: Nature 403, 853–858. DOI: 10.1038/35002501

NASA (National Aeronautics and Space Administration) (2005): Shuttle Radar Topography Mission. Imagenes SRTM de America del Sur. http://www2.jpl.nasa.gov/srtm/southAmerica_sp.htm (Date: 25.06.2015)

NOAA-CLASS (2015): NOAA's Comprehensive Large Array-data Stewardship System (CLASS). http://www.class.noaa.gov (Date: 25.06.2015)

Nonomura, A.; Sanga-Ngoie, K. and Fukuyama, K. (2003): Devising a new digital vegetation model for eco-climatic analysis in Africa using GIS and NOAA AVHRR data. In: International Journal of Remote Sensing 24, 3611–3633. DOI: 10.1080/0143116021000053779

Olander, L. P.; Gibbs, H. K.; Steininger, M.; Swenson, J. J. and Murray, B. C. (2008): Reference scenarios for deforestation and forest degradation in support of REDD: a review of data and methods. In: Environmental Research Letters 3 025011. DOI: 10.1088/1748-9326/3/2/025011

Ochoa-Cueva, P.; Fries, A.; Montesinos, P.; Rodríguez-Díaz, J. A. and Boll, J. (2015): Spatial estimation of soil erosion risk by land-cover change in the Andes of Southern Ecuador. In: Land Degradation & Development 26, 565–573. DOI: 10.1002/ldr.2219

Poulter, B.; Hattermann, F.; Hawkins, E. D.; Zaehle, S.; Sitch, S.; Restrepo-Coupe, N.; Heyder, U. and Cramer, W. (2010): Robust dynamics of Amazon dieback to climate change with perturbed ecosystem model parameters. In: Global Change Biology 16, 2476–2495. DOI: 10.1111/j.1365-2486.2009.02157.x

Puyravaud, J. P. (2003): Standardizing the calculation of the annual rate of deforestation. In: Forest Ecology and Management 177, 593–596. DOI: 10.1016/S0378-1127(02)00335-3

Quorum Communications (2015): Satellite Remote Sensing Systems & Electronics. http://www.qcom.com/ (Date: 20.05.2015)

Richter, M. (2003): Using epiphytes and soil temperatures for eco-climatic interpretations in southern Ecuador. In: Erdkunde 57 (3), 161–181. DOI: 10.3112/erdkunde.2003.03.01

Roderick, M.; Smith, R. and Lodwick, G. (1996): Calibrating long-term AVHRR-derived NDVI imagery. In: Remote Sensing of Environment 58, 1–12. DOI: 10.1016/0034-4257(96)00035-1

Saatchi, S. S.; Harris, N. L.; Brown, S.; Lefsky, M.; Mitchard, E.; Salas, W.; Zutta, B. R.; Buermann, W.; Lewis, S. L.; Hagen, S.; Petrova, S.; White, L. and Morel, A. (2011): Benchmark map of forest carbon stocks in tropical regions across three continents. In: Proceedings of the National Academy of Science of the United States of America 108, 9899–9904. DOI: 10.1073/pnas.1019576108

Simic, A.; Fernandes, R.; Brown, R.; Romanov, P. and Park, W. (2004): Validation of VEGETATION, MODIS, and GOES + SSM/I snow-cover products over Canada based on surface snow depth observations. In: Hydrological Processes 18, 1089–1104. DOI: 10.1002/hyp.5509

Tan, K.; Piao, S.; Peng, C. and Fang, J. (2007): Satellite-based estimation of biomass carbon stocks for northeast China's forests between 1982 and 1999. In: Forest Ecology and Management 240, 114–121. DOI: 10.1016/j.foreco.2006.12.018

Tapia-Armijos, M. F.; Homeier, J.; Espinosa, C. I.; Leuschner, C. and de la Cruz, M. (2015): Deforestation and forest fragmentation in South Ecuador since the 1970s – losing a hotspot of biodiversity. In: PLOS ONE 10. DOI: 10.1371/journal.pone.0133701

Thomas, C. D.; Cameron, A.; Green, R. E.; Bakkenes, M.; Beaumont, L. J.; Collingham, Y. C.; Erasmus, B. F. N.; Ferreira de Siqueira, M.; Grainger, A.; Hannah, L.; Hughes, L.; Huntley, B.; van Jaarsveld, A. S.; Midgley, G. F.; Miles, L.; Ortega-Huerta, M. A.; Townshend Peterson, A.; Phillips, O. L. and Williams, S. E. (2004): Extinction risk from climate change. In: Nature 427, 145–148. DOI: 10.1038/nature02121

Thuiller, W. (2007): Biodiversity: climate change and the ecologist. In: Nature 448, 550–552. DOI: 10.1038/448550a

Tucker, C. J.; Pinzon, J. E.; Brown, M. E.; Slayback, D.; Pak, E. W.; Mahoney, R.; Vermote, E. and El Saleous, N. (2005): An extended AVHRR 8-km NDVI data set compatible with MODIS and SPOT Vegetation NDVI data. In: International Journal of Remote Sensing 26, 4485–4498. DOI: 10.1080/01431160500168686

Wang, L.; Xiao, P.; Feng, X.; Li, H.; Zhang, W. and Lin, J. (2014): Effective compositing method to produce cloud-free AVHRR image. In: IEEE Geoscience and Remote Sensing Letters 11, 328–332. DOI: 10.1109/LGRS.2013.2257672

WorldClim (2015): Global Climate Data – Free climate data for ecological modeling and GIS. http://www.worldclim.org (Date: 25.06.2015)

Wunder, S. (2000): The economics of deforestation: the example of Ecuador. London.

Yoshikawa, S. and Sanga-Ngoie, K. (2011): Deforestation dynamics in Mato Grosso in the southern Brazilian Amazon using GIS and NOAA/AVHRR data. In: International Journal of Remote Sensing 32, 523–544. DOI: 10.1080/01431160903475225

Zhang, X.; Friedl, M. A.; Schaaf, C. B.; Strahler, A. H.; Hodges, J. C. F.; Gao, F.; Reed, B. C. and Huete, A. (2003): Monitoring vegetation phenology using MODIS. In: Remote Sensing of Environment 84, 471–475. DOI: 10.1016/S0034-4257(02)00135-9

Authors

Víctor González-Jaramillo
Departamento de Geología y Minas
e Ingeniería Civil (DGMIC)
Grupo de trabajo de Hidrología y
Climatología
Universidad Técnica Particular de
Loja
San Cayetano Alto
Loja
Ecuador
and
LCRS, Department of Geography
Faculty of Geography
University of Marburg
Deutschhausstr. 10
35032 Marburg
Germany
vhgonzalez26@gmail.com

Dr. Andreas Fries
Departamento de Geología y Minas
e Ingeniería Civil (DGMIC)
Grupo de trabajo de Hidrología y
Climatología
Universidad Técnica Particular de
Loja
San Cayetano Alto
Loja
Ecuador
and
LCRS, Department of Geography
Faculty of Geography
University of Marburg
Deutschhausstr. 10
35032 Marburg
Germany

PD Dr. Rütger Rollenbeck
LCRS, Department of Geography
Faculty of Geography
University of Marburg
Deutschhausstr. 10
35032 Marburg
Germany

Jhoana Paladines
Dirección de Materiales y Recursos Educativos
Universidad Técnica Particular de Loja
San Cayetano Alto
Loja
Ecuador

Dr. Fernando Oñate-Valdivieso
Departamento de Geología y Minas e Ingeniería
Civil (DGMIC)
Grupo de trabajo de Hidrología y Climatología
Universidad Técnica Particular de Loja
San Cayetano Alto
Loja
Ecuador

Prof. Dr. Jörg Bendix
LCRS, Department of Geography
Faculty of Geography
University of Marburg
Deutschhausstr. 10
35032 Marburg
Germany

Regional forest cover of the years 1986, 2001 and 2008

Coastal Lowland (6 554 000 ha)

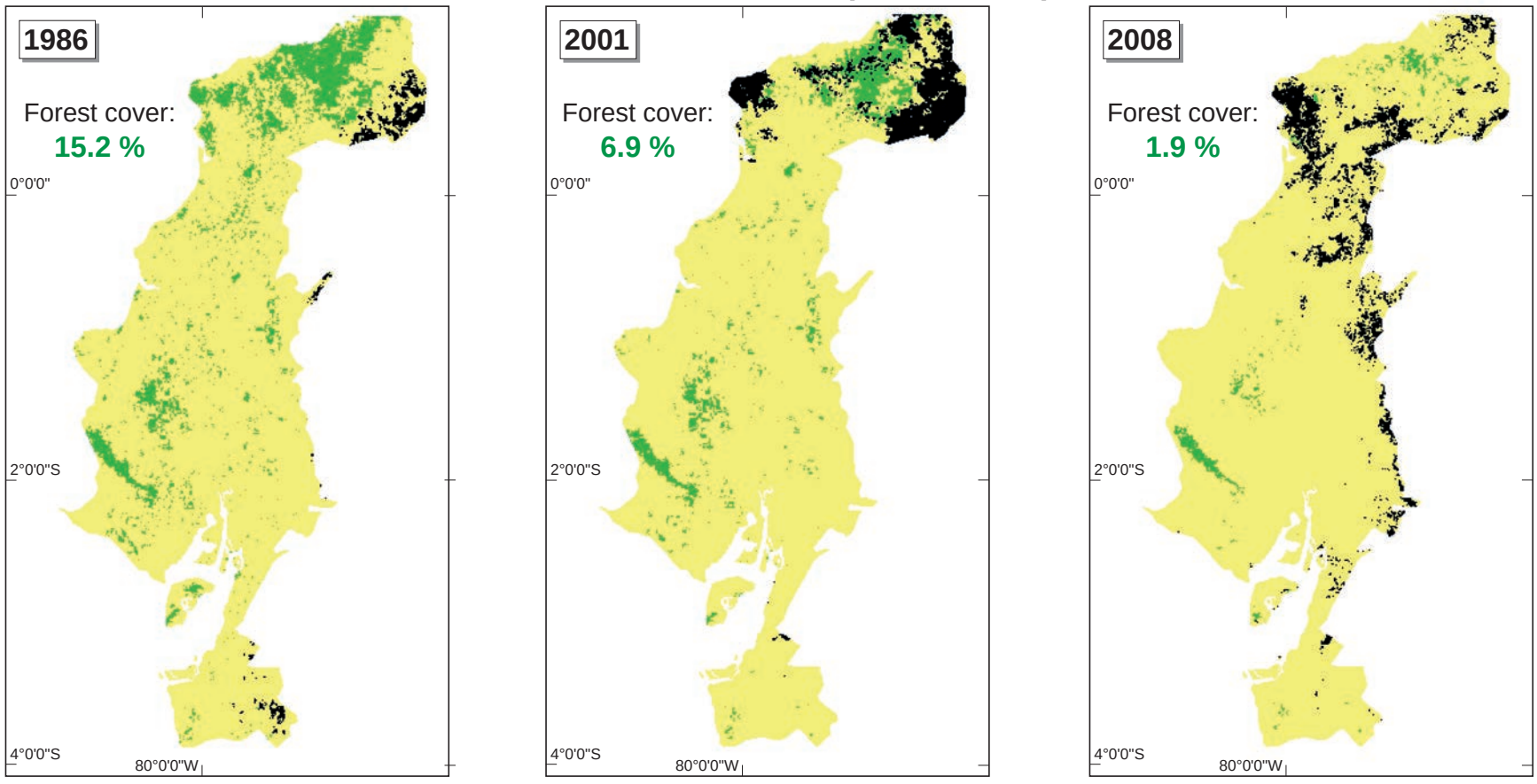

Andean Highland (6 474 900 ha)

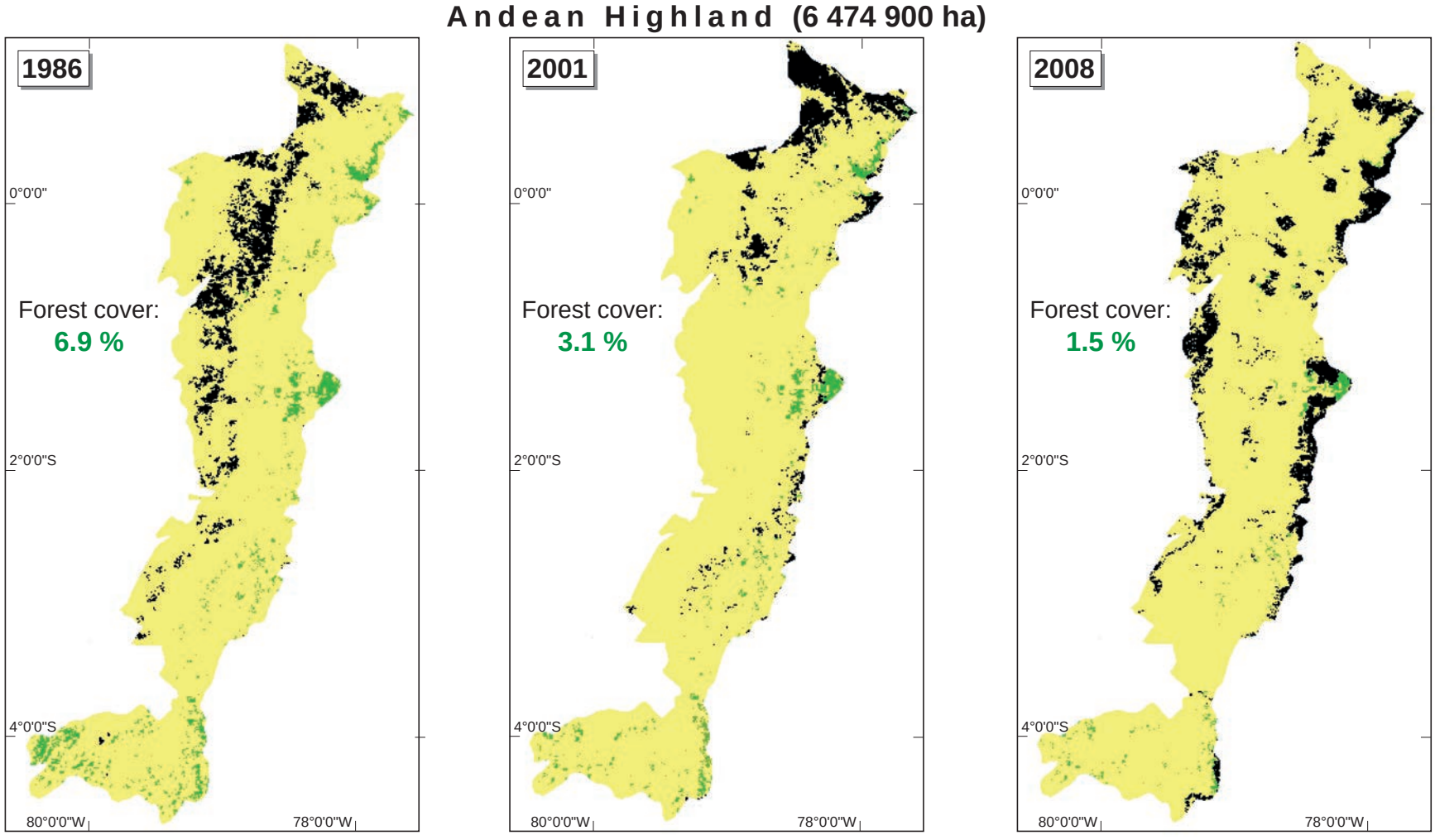

Amazon Basin (11 630 100 ha)